negligible. In the case of normal impingement $\alpha = \pi/2$, the force normal to the plane is

$$F = \rho q^2 A \quad (1)$$

The thickness of the deflected jet flow along the plane, at distance r from central impingement point O, is given by symmetry as

$$a(r) = \frac{A}{2\pi r} \quad (2)$$

Equation (1) expresses momentum conservation, while (2) is a statement of continuity in an incompressible fluid, ρ being constant.

When the jet axis is not normal to the plane, $\alpha < \pi/2$ and axial symmetry is replaced by plane symmetry. Cartesian coordinates x and y in the flat boundary surface are introduced with origin at O, x counted positive in the direction of forward-moving flow in the symmetry plane, y perpendicular to x. An azimuth angle β in the x,y plane is defined by the equations

$$x = r\cos\beta \qquad y = r\sin\beta$$

and the thickness of the deflected jet at any place can be written $a(r,\beta;\alpha)$; in this notation the expression (2) becomes $a(r,\beta;\pi/2)$.

Momentum flux consideration normal to the x,y plane shows that the force exerted between jet and wall is

$$F = \rho q^2 A \sin\alpha \quad (3)$$

independent of the form of the deflected jet given by $a(r,\beta;\alpha)$. For the determination of this quantity, the continuity condition analogous to (2) gives

$$\int_0^{2\pi} a(r,\beta;\alpha)\, r\, d\beta = A \quad (4)$$

and momentum arguments provide two additional relationships.

There is no force in the x-direction, and the net outward flux of x-momentum through a suitably chosen control volume is zero, so that

$$\int_0^{2\pi} \rho q\, a(r,\beta;\alpha)\, r\, d\beta\, q\cos\beta = A\rho q^2\cos\alpha \quad (5)$$

The momentum balance in the y-direction likewise gives

$$\int_0^{2\pi} \rho q\, a(r,\beta;\alpha)\, r\, d\beta\, q\sin\beta = 0 \quad (6)$$

expressing the symmetry already mentioned. The four equations (3), (4), (5) and (6) represent all of the conditions imposed by the conservation laws, and any meaningful solution $a(r,\beta;\alpha)$ must satisfy these equations. The same four equations are not sufficient to determine $a(r,\beta;\alpha)$ uniquely, however. A solution seen by inspection which reduces to (2) in the limit $\alpha = \pi/2$ is

$$a(r,\beta;\alpha) = \frac{A}{2\pi r}(1 + 2\cos\beta\cos\alpha) \quad (7)$$

The function given by (7) can be regarded as the leading terms of a Fourier cosine series neglect of higher harmonics being justified by consideration of surface tension effects, for example.

β values in the interval $(\pi/2, 3\pi/2)$ identify fluid particles the x-momenta of which are reversed by impingement, the entire region representing backflow. It is seen from equation (7) that the thickness of the backflow jet is smaller than in the region of forward-deflected flow. The same is true for flat jets, but a peculiar feature of the present three-dimensional jet is seen as α decreases to the value $\pi/3$, when the thickness of the jet approaches zero as β approaches π, that is, along the negative x-axis. For still smaller values of the impingement angle α, the thickness a reaches zero at values of $\beta < \pi$, forming a wedge-shaped zone that increases in size as $\alpha \to 0$, when a limiting "dry zone" wedge angle $\pi/3$ is attained. (Note that the avoidance of negative values of $a(r,\beta;\alpha)$ depends on retaining harmonics not written in equation (7).) The occurrence of a dry zone contrasts with the case of the flat jet for which the thickness of the backflow region decreases steadily with α, as $\sin^2\alpha/2$, reaching zero only when $\alpha = 0$.

The physical interpretation is that the lateral flow deflexion occurring in the three-dimensional jet flow furnishes an alternative relief for the overpressures in the vicinity of the central impingement point O, reducing the requirement for rearward splash at sufficiently small impingement angles.

IRVING MICHELSON

Department of Aerospace Engineering,
Illinois Institute of Technology,
Chicago 60616.

Received April 21; revised June 20, 1969.

[1] Lamb, H., *Hydrodynamics*, sixth ed. (Dover Publications, 1945).
[2] Ginsburg, I. P., *Applied Fluid Dynamics*, Izdatel'stvo Leningradskogo Universiteta, 1958 (also issued as NASA TT F-94, 1963).
[3] Gurevich, M. I., *Theory of Jets in Ideal Fluids* (Academic Press, 1965).

Evaporated Silver Bromide as an Ion and Particle Detector

A GELATINE emulsion of silver bromide grains is the universal detector for most radiations and is described by a vast literature[1]. It is, however, possible to produce radiation-sensitive thin films (0·2–0·6 microns) of pure silver bromide by vacuum evaporation[2–7]. The applications of such thin films to particle beam detection are discussed here.

In the familiar emulsion, the sensitometric curve of average density versus exposure and the granularity are both predictable by a statistical model which depends on available knowledge of grain size distribution and number of grains made developable per impacting particle. This is possible because (1) the grains are small and numerous enough spatially to "resolve" the Poisson distributed fluctuations of the radiation and to allow the application of binomial statistics of the grains to the spatial density fluctuations; (2) the developed and undeveloped grain sizes are related, and the probability of developing an unexposed grain (fog) even in the vicinity of exposed grains (infectious development) is usually small.

An equivalent model does not exist for a thin continuous film of AgBr. Although electron micrographs show bounded contiguous regions or domains[4], there is no evidence that these domains are physically isolated. During exposure, the diffusion of photoelectrons and photoholes into unexposed regions is therefore a consideration. Furthermore, enhancement of development activity in regions of high latent image density may cause unexposed adjacent domains to undergo development. In such a grainless system one cannot relate the observed granularity to the statistics of a distribution of grains nor would one expect the microscopic character of developed density to be influenced by the statistics of the exposure.

Because these AgBr films are unsensitized they have negligible sensitivity to light of wavelength longer than 0·5 microns and are not useful for most common optical photographic recording applications. In beams exceeding 1 kV, however, the particles are at least two orders of magnitude more energetic than visible light photons—sufficient to render a struck emulsion grain developable. Because the AgBr evaporated layer presents a bare continuous surface free of gelatine, it is of interest as a particle detector, especially for particles such as large organic

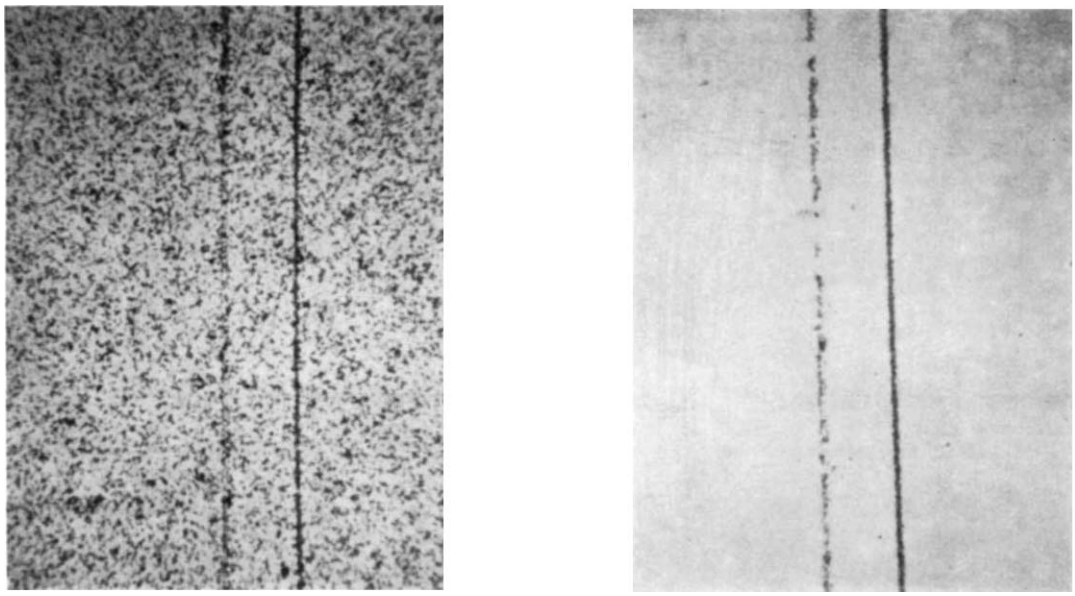

Fig. 1. Comparison of signal/noise at threshold of detection in the mass spectra of an organic mixture, mass 92–93. The exposure on the left was made with a conventional plate and the one on the right was made with an evaporated AgBr plate.

ions and low energy electrons that have a small penetrating range in gelatine[8,9].

The surface of evaporated AgBr has been studied by electron microscopy and X-ray diffraction. The former shows that a continuous surface of 0·3 micron domains occurs when a film thickness of 0·15 microns is attained. In the growth and agglomeration of crystallites, the dominant orientation is found to change from (111) to (100) (ref. 2), the latter predominating in the thickness range of 0·15–0·5 microns.

Vapour deposition of AgBr causes decomposition in the melt which produces gaseous bromine. Bromine reduces detection sensitivity if it is absorbed in the evaporated layer. Outgassing the surface at 150° to 200° C restores sensitivity, however. The increased surface energy resulting from this heating roughly doubles the size of the crystal domains.

If evaporated AgBr samples are illuminated uniformly, the resulting free silver formation may be studied from a series of partially developed samples[4]. We find the contiguous domain structure prone to infectious development. The technique used for controlling unbounded silver formation is the use of an "internal" developer containing an AgBr solvent. Although the solvent component may dissolve some surface latent image, it adds depth to the domain boundaries. The reduction to free silver is initially in the domain boundaries (where development activity is apparently greatest), and infection is primarily by filamentary silver growth along domain boundaries which, however, may cause the development of adjacent unexposed domains. When development nears completion, the filamentary silver seems to grow into the domain regions, indicating a loss of any correlation between the silver image and the pre-development domain structure.

The maximum obtainable opaque silver coverage produced by particle beam exposure is approximately 99 per cent, or density 2, which is quite high considering that the AgBr deposit is a single sub-micron layer. The exposure range from the threshold of detection to saturation is typically one order of magnitude, generating a steep sensitometric curve of $\gamma > 2$. Factors contributing to this relatively small latitude are the presence of only one registration layer and the tendency for regions of heavy exposure to be overdeveloped. Greater latitude can be obtained by underdevelopment or by increasing the solvent component of the developer. The latter suppresses overdevelopment by simultaneously removing unreduced AgBr, but this causes a subsequent reduction in maximum density.

As in lenses, the resolution or bandwidth of film is often stated in terms of an MTF (modulation transfer function). The MTF may be obtained as the normalized modulus of the Fourier transform of a "spread" function, which is the film's response to a spatial impulse such as an edge or point exposure. (Though impractical in the case of particle exposures, the MTF may also be generated directly as the contrast ratio resulting from a sine wave exposure of varying spatial frequency.) While valid for optical systems the MTF is questionable in the case of photographic film, and particularly evaporated AgBr, because of the non-linear development process whereby the spread function's shape is not generally independent of the magnitude of the impulse. Evaporated AgBr suffers the additional vulnerability of exposure dependent non-linear image spreading during exposure. Also the MTF analysis does not usually include the contribution to signal degradation by statistical density fluctuations. Such noise can be filtered, for example, by the averaging effect of scanning a long edge image by a long densitometer slit, or mathematical methods. The resulting MTF may therefore indicate a bandwidth which is effectively exaggerated. This is likely to be true for evaporated AgBr where in the case of electron beam recording, for example, granularity is greater than in conventional films.

Because of these limitations, estimates of evaporated AgBr resolution obtained directly from test targets of appropriate contrast and configuration are more meaningful than an MTF calculation. As an example, from an edge produced by electron beam exposure separating regions with a density difference of 0·5 units the half width of the image of the edge indicates the ability of evaporated AgBr to resolve at approximately 5 microns with an improvement in resolution expected for a smaller density difference. This resolution value, equivalent to roughly 200 l/mm, falls short of what might ideally be expected from a sub-micron thick layer because of the spreading effects already mentioned.

Detectivity in an exposure area A is noise (granularity) dependent. Symbolically $S = g(\bar{D})/A\sigma(\bar{D},A)$, where S is

sensitivity to detect small differences in signal, σ is the standard deviation from average density $\bar{D}$ due to random density fluctuations and g is the slope of the film's sensitometric curve. The S_{max} usually occurs at a moderate exposure value between the knee and toe of the sensitometric curve. For optimum detection of a weak signal, then, the film must be "biased" by a much stronger uniform background flux ensuring the condition $S = S_{max}$ on a region of the film including A. Biasing may be impractical in cases where information is carried by neighbouring weak and strong signals, as in mass spectrometry.

In these cases, weak signal detection is limited by fog level. For a granular emulsion, the number of developed grains per unit area produced by a weak particle beam divided by the number of fog grains per unit area approximates the signal-to-noise ratio. Although the same criterion applies for evaporated AgBr (with the stipulation that silver filaments are not developed AgBr grains, but result from spreading phenomena associated with exposure and development) important differences between the granular emulsion and evaporated AgBr film exist.

These differences become apparent when an emulsion designed for particle detection and evaporated AgBr are both exposed to about 10^7 particles/cm^2. Such an exposure produces a developed grain count on the emulsion of about 5× above fog—allowing a count of individual struck grains using a medium power microscope. In an experiment where 15 kV electrons strike the emulsion, better than half the electrons register. In a similar exposure of evaporated AgBr film, the registration efficiency seems to be much lower. That is, even though the AgBr layer is continuous, there are larger but fewer isolated silver specks. (A meaningful estimate of registration is precluded by the lack of silver speck isolation.) Although registration appears less efficient, the fog level of evaporated AgBr is very low. If therefore the loss of registration on evaporated AgBr can be compensated for by prior knowledge of the exposure configuration, then a signal/noise advantage may exist over emulsion films that generally have a much greater fog level. (For example, prior knowledge allows recognition of a weak spectral line from a few isolated colinear silver specks against a clear background). Such a signal/noise advantage is shown in Fig. 1 where an ion emulsion plate and an evaporated AgBr plate are subjected to the same electronically measured ion exposure. If, in this comparison, the exposure level is reduced (not shown), the weak line image on the evaporated AgBr surface can still be detected by optical microscopy but is lost on the conventional emulsion plate.

Thus in threshold detection using very low fog evaporated AgBr, the readout system rather than fog may be the principal noise source. In normal densitometer conditions, a very weak exposure on evaporated AgBr is likely to be below densitometer noise and therefore not detectable. On the other hand, such a low density image consisting of a few Ag specks may be found against an extremely low background fog level by visual observation through a microscope.

A heavy exposure on film is invariably accompanied by flare, presumably due to registration of the low level part of a radiation pattern not detectable in normal exposures. In such conditions, reversal phenomena caused by excessive bromine (positive hole) concentration in the process of latent image formation are often observed[10]. In the gelatine emulsion, bromination effects are suppressed by two mechanisms not normally available in evaporated AgBr film. First, the dispersion of the sensitive material as small isolated grains creates a large surface/volume ratio favourable to bromine release at the grain surface. Second, the gelatine behaves as a bromine acceptor, enhancing the escape of bromine atoms and preventing their spread to neighbouring grains. Evaporated AgBr, on the other hand, with its continuous binder-free layer of relatively low surface/volume ratio,

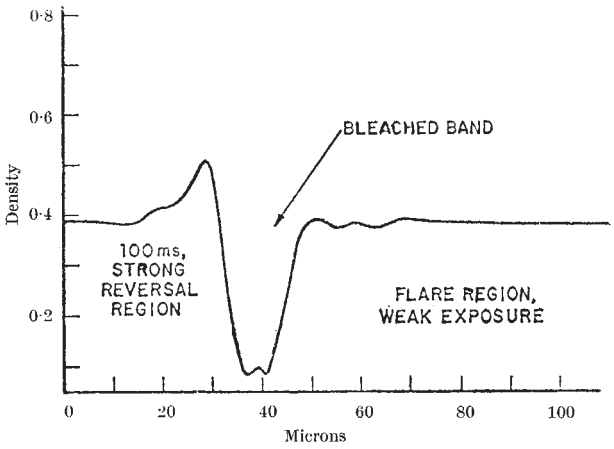

Fig. 2. Edge trace of erased band surrounding a heavy exposure.

is vulnerable to recombination. The following observations are consistent with recombination assumptions: dramatic density reduction within the region of exposure for exposures above saturation, and the erasing and desensitizing of regions surrounding a heavy exposure. These observations are illustrated by the trace of a heavy electron beam edge exposure (Fig. 2). The exposure region (left) has reversed to 1/4 maximum density and a bleached band exists to the right, in the flare of the adjacent shadow region. If before development this edge is re-exposed with a normal exposure (that by itself would produce maximum density) only the flare region is effected, its density increasing to $D \simeq 2$. The reversal region and the bleached band are unaffected, indicating that the bleached band is also a desensitized band.

In particular, these erased and desensitized bands, the width of which increases with exposure, strongly suggest bromination by highly mobile positive holes generated within the heavy exposure region in numbers too great to preclude diffusion to surrounding areas. The diffusion argument is also supported in Fig. 2 by evidence of a gradient in the number density of the diffusing species; that is, a reduction of the positive hole concentration due to diffusion into the flare region would allow a local density increase on the heavy exposure side of the edge. This is shown by the density peak in Fig. 2. Further study is required to establish that the erased bands are clear cut evidence supporting the bromination theory of reversal. Their desensitization to a re-exposure virtually eliminates development as the origin of the phenomenon, however.

We conclude that evaporated AgBr film exhibits striking phenomena relevant to both the study of latent image formation and recombination effects.

JOSEPH I. MASTERS

Technical Operations Incorporated,
South Avenue,
Burlington, Massachusetts 01803.

Received November 29, 1968; revised June 4, 1969.

[1] Mees, C. E. K., *The Theory of the Photographic Process* (Macmillan Co., New York, 1954).
[2] Hirata, A., and Tsunoko, Y., *Nippon Shashin Gokkai Kaishi*, **28**, 38 (1965).
[3] Honig, R. E., Woolston, J. R., and Kramer, D. A., *Rev. Sci. Instrum.*, **38** (12), 1703 (1967).
[4] Shepp, A., Whitney, R., and Masters, J., *Phot. Sci. Eng.*, **11**, 322 (1967).
[5] Bazinet, M., and Masters, J., *Trans. Mass Spectrometer Conf. Denver G-19* (May 1966).
[6] Hunt, M., *Analytic Chem.*, **38**, 620 (1966).
[7] Shepp, A., Goldberg, G., Masters, J., and Lindstrom, R., *Phot. Sci. Eng.*, **11** (5), 316 (1967).
[8] Watanake, E., Naito, M., and Shino, N., *Seventeenth Ann. Conf. Mass Spectrometry*, Dallas, Texas (May 1969).
[9] Masters, J., *Conf. on Mass Spectrometric Analysis of Solids* (National Bureau of Standards, Washington, DC, November 1968).
[10] Mees, C. E. K., *The Theory of the Photographic Process*, 147 (Macmillan Co., New York, 1954).